

The Role of Phase Contrast MRI in Studying Cerebrospinal Fluid Dynamics in Relevant Pathologies

Essay

Submitted for the Partial Fulfilment of
Master Degree of Radiodiagnosis

By

Maram Mahmoud Gamal Tawfik
M.B.B.Ch,

Supervised by

Prof. Dr. Mounir Sobhy Guirguis

Professor of Radiodiagnosis
Faculty of Medicine
Ain Shams University

Dr. Rania Mohammed Refaat Abd El Hamid

Lecturer of Radiodiagnosis
Faculty of Medicine
Ain Shams University

Faculty of Medicine

Ain Shams University

2013

Acknowledgement



First of all, I thank Allah for all his blessings and care, that helped me finish this work.

I would like to express my thanks and deep gratitude to **Prof. Dr. Mounir Sobhy Guirguis** Professor of Radiodiagnosis, Faculty of Medicine, Ain Shams University, for his guidance, advice and thoughtful remarks.

Also I would like to express my thanks and appreciation to **Dr. Rania Mohammed Refaat Abd El Hamid** Lecturer of Radiodiagnosis, Faculty of Medicine, Ain Shams University, for his continuous encouragement, help and valuable comments.

Last but not least, I would like to thank my family for their help and encouragement and I would like to dedicate this work to them.

List of Contents

Title	Page No.
<i>Introduction</i>	<i>10</i>
<i>Aim of the Work</i>	<i>12</i>
<i>Anatomical and Physiological Basis for CSF Pathway.....</i>	<i>13</i>
<i>Physical Principle of Phase Contrast MRI.....</i>	<i>45</i>
<i>Different Pathologies Affecting CSF Flow</i>	<i>66</i>
<i>Phase Contrast MRI Manifestations of Different Pathologies Affecting CSF Flow with Illustrative Cases.....</i>	<i>101</i>
<i>Summary and Conclusion.....</i>	<i>124</i>
<i>References</i>	<i>127</i>
<i>Arabic Summary</i>	

List of Tables

Table No.	Title	Page No.
-----------	-------	----------

Table (1): Traditional theories of pathogenesis of hydrocephalus. 69

Table (2):.....Causes and sites of obstruction 73

Table (3):.....Indications for ETV divided into two groups 81

Table (4):.....Sites of arachnoid cysts. 91

List of Figures

Fig. No.	Title	Page No.
Figure (1):	Ventricles of the brain. Labels" R.SP. recessus suprapinealis	14
Figure (2):	Coronal section through the frontal lobes and the anterior horns of the lateral ventricle	15
Figure (3):	Dissection, to show the fornix and the posterior and descending cornua of the lateral ventricle	16
Figure (4):	Dissection, to show the posterior and descending cornua of the lateral ventricle hippocampus	17
Figure (5):	Coronal illustration of the right temporal lobe showing the optic radiation isolated from the lateral ventricle	18
Figure (6): Illustration of the anatomy of the third ventricle	20
Figure (7): Anatomy of the third ventricle	21
Figure (8):	Normal anatomy of the cerebral aqueduct as viewed in the sagittal plane	23
Figure (9):Sagittal section showing fourth ventricle	25
Figure (10):	Sagittal section of the brain illustrating the positions of the principal subarachnoid spaces	26
Figure (11):	Coronal section through the vertex of the skull showing the relationships between the lateral ventricle and the third ventricle	27
Figure (12): Axial T2 MRI image showing lateral ventricle	30
Figure (13): Axial T2 MRI image showing body of lateral ventricle	30
Figure (14):	Axial T2 MRI image showing temporal horn of lateral ventricle	31
Figure (15): Sagittal T2 MRI image showing body of lateral ventricle	31

List of Figures (Cont...)

Fig. No.	Title	Page No.
Figure (16):	Coronal T2 MRI showing occipital horn of lateral ventricle	32
Figure (17): Axial T2 MRI image showing Third Ventricle	33
Figure (18):	Sagittal T2 MRI showing Third, Fourth Ventricle and cerebral aqueduct	33
Figure (19): Coronal T2 MRI image showing Third Ventricle	34
Figure (20): Axial T2 MRI image showing cerebral aqueduct	34
Figure (21): Axial T2 MRI image showing 4th ventricle	35
Figure (22): CSF drainage pathways	39
Figure (23):	Showing piston like remodeling of brain structures during systole	41
Figure (24):	Diagrams show that spins moving along an external magnetic field gradient acquire a phase shift	42
Figure (25):	Diagram shows that two acquisitions are performed, each one with all parameters	43
Figure (26): Normal CSF flow in the sagittal plane.	54
Figure (27):	(a) Sagittal T1W MR image shows the phase-contrast imaging plane to assess aqueductal flow	55
Figure (28):	Axial phase-contrast images obtained perpendicular to the aqueduct.	56
Figure (29):	(A) Sagittal reference image with axial section perpendicular to the spinal canal at the level of the aqueduct	57

List of Figures (Cont...)

Fig. No.	Title	Page No.
Figure (30):	The midline sagittal T1-weighted MRI study is used to graphically describe the ph	
Figure (31):	Midline sagittal T2-weighted image showing the positions of the localizers for the	
Figure (32): Graph depicting the CSF flow waveform.	58
Figure (33):	Midsagittal phase-contrast images(a) end of CSF diastole,(b) CSF systole,(c) CSF r	
Figure (34): Curves shows CSF dynamics during one cardiac cycle.	62
Figure (35):	Axial T1-weighted image shows Primary monoventricular hydrocephalus	71
Figure (36):	Gd-enhanced sagittal T1-weighted image shows Tetra ventricular hydrocephalus	
Figure (37):	Gd-enhanced sagittal T1-weighted image shows communicating hydrocephalus, 75	
Figure (38): Sagittal T2-weighted image shows aqueductal stenosis	79
Figure (39):	Postoperative MRI scan of a patient shows the fenestration site in ETV and flow v	
Figure (40):	Sagittal T2-weighted image shows Chiari I malformation, note that the vermis (V)	
Figure (41): The anatomy of a Chiari I malformation	86
Figure (42): A: Coronal T2-weighted image, B: Axial FLAIR image..	91
Figure (43): Illustration of intracranial arachnoid cyst location	92
Figure (44): Cystic malformations of the posterior fossa	94
Figure (45): Dandy-Walker malformation	95

List of Figures (Cont...)

Fig. No.	Title	Page No.
Figure (46): Dandy-Walker variant	96
Figure (47): Minor form of Dandy-Walker variant	97
Figure (48): The Blake's pouch.	98
Figure (49): Persistent Blake's pouch	99
Figure (50): Mega cisterna magna	100
Figure (51): Aqueductal CSF flow velocity of NPH.	104
Figure (52):	Comparison of CSF flow dynamics before and after VP shunt in the NPH group. 10	
Figure (53): Complete aqueductal stenosis and hydrocephalus.	107
Figure (54):	A, Sagittal T1-weighted image obtained before the third ventriculostomy. Large la	
Figure (55):	A 20-year-old man with headaches and a communicating left middle cranial fossa	
Figure (56): A left middle cranial fossa cyst 1 week after surgery	112
Figure (57):	Phase-contrast MR images of Chiari I patient show restricted CSF flow	114
Figure (58):	Color and surface plot images of CSF flow velocity in the foramen magnum of Chia	

Figure (59):	Quantitative phase-contrast image shows a delayed peak velocity position and pro	
Figure (60): Cervical syringomyelia	118
Figure (61):Pre- and postoperative evolution.	119
Figure (62):	Dandy walker malformation (A) T2-w axial image, (B) T1-w sagittal image,(C) pha	

List of Figures *(Cont...)*

Fig. No.	Title	Page No.
Figure (63):	A 3-month-old infant with multiple congenital anomalies examined by cranial MR	
Figure (64):	A 20-year-old male with the diagnosis of persistent BPC presented with vertigo an	
Figure (65):	An 18-year-old male with the diagnosis of MCM presented with headache	12

List of Abbreviations

Abb.	Full term
<i>AC</i>	<i>Arachnoid cysts</i>
<i>ACSV</i>	<i>Aqueductal CSF stroke volume</i>
<i>AS</i>	<i>Aqueductal stenosis</i>
<i>BPC</i>	<i>Persistent Blake's pouch</i>
<i>CECT</i>	<i>Contrast enhanced computed tomography</i>
<i>CTC</i>	<i>Computed tomography cisternography</i>
<i>CIM</i>	<i>Type I Chiari malformation</i>
<i>CIIM</i>	<i>Type II Chiari malformation</i>
<i>CSF</i>	<i>Cerebrospinal fluid</i>
<i>CT</i>	<i>Computed tomography</i>
<i>DWM</i>	<i>Dandy-Walker malformation</i>
<i>DMV</i>	<i>Dandy-Walker variant</i>
<i>ECG</i>	<i>Electrocardiography</i>
<i>ETV</i>	<i>Endoscopic third ventriculostomy</i>
<i>FLAIR</i>	<i>Fluid attenuation inversion recovery</i>
<i>FLASH</i>	<i>Fast low angle shot</i>
<i>Gd</i>	<i>Gadolinium</i>
<i>GRE</i>	<i>Gradient recalled echo</i>
<i>HR</i>	<i>Heart rate</i>
<i>ICP</i>	<i>Intracranial pressure</i>
<i>MCM</i>	<i>Mega cisterna magna</i>
<i>MRI</i>	<i>Magnetic resonance imaging</i>
<i>NECT</i>	<i>Non enhanced computed tomography</i>
<i>NEX</i>	<i>Number of excitations</i>
<i>NPH</i>	<i>Normal pressure hydrocephalus</i>
<i>PC-MRI</i>	<i>Phase contrast magnetic resonance imaging</i>
<i>PD</i>	<i>Proton density</i>

PSV Peak systolic velocity
PDV Peak diastolic velocity
R-D Time after R wave to onset of CSF diastole.
ROI Region of interest
R-PDV R-wave to peak diastolic velocity.
R-PS Time after R wave to peak of CSF systole
R-S Time after R wave to onset of CSF systole
SDFC Subdural fluid collection
SNR Signal to noise ratio
SV Stroke volume
TE Echo time
TR Repetition time
Venc Velocity encoding
VP shunt Ventriculoperitoneal shunt
2D 2 dimensions
3D 3 dimensions

INTRODUCTION

The Cerebrospinal Fluid (CSF) flow is influenced by two separate processes; the circulation of the CSF from its formation sites to its absorption sites (i.e., bulk flow) and an oscillatory (back and forth) flow during the cardiac cycle (pulsatile flow) (*Alperin et al., 2006*). Phase contrast MRI non invasively displays this pulsatory CSF motion and allows assessment of its amplitude (*Bhadelia et al., 1997*).

Cine phase contrast MRI has many advantages other than non invasiveness including no need for patient preparation or contrast media injection, no ionizing radiation exposure and overall examination duration less than 15 min (*Unal et al., 2009*). Moreover, it is extremely sensitive, even to slow flow (*Schroeder et al., 2000*).

Phase contrast MR flow studies can be used as a selective noninvasive method for establishing the diagnosis of normal pressure hydrocephalus (*Al-Zain et al., 2008*), to discriminate between communicating hydrocephalus and non communicating hydrocephalus, to localize the level of obstruction in obstructive hydrocephalus, to differentiate between arachnoid cysts and subarachnoid space enlargement and to determine whether arachnoid cysts communicate with the subarachnoid space (*Yildiz et al., 2006*).

Cine phase-contrast MR imaging for CSF flow evaluation may be a useful adjunct to routine MR imaging in the evaluation of the cystic malformations of the posterior fossa because it can improve the specificity in differentiating such malformations (*Yildiz et al., 2006*). Phase contrast cine MR imaging is considered a reliable method for evaluating the patency of a third ventriculostomy (*Fukuhara et al., 1999*) and has been adopted for the assessment of CSF flow in a variety of disorders including Chiari I malformation and syringomyelia (*Wentland et al., 2010*).

AIM OF THE WORK

Aim of this work is to emphasize the role of phase contrast MRI in evaluation of CSF flow in relevant pathologies.

ANATOMICAL AND PHYSIOLOGICAL BASIS FOR CSF PATHWAY

A- The anatomy of ventricular system:

The cerebral ventricular system consists of a series of interconnecting spaces and channels within the brain (*Figure 1*) which are derived from the central lumen of the embryonic neural tube and the cerebral vesicles to which it gives rise:

- Two lateral ventricles.
- Third ventricle.
- Fourth ventricle (*Crossman, 2005*).

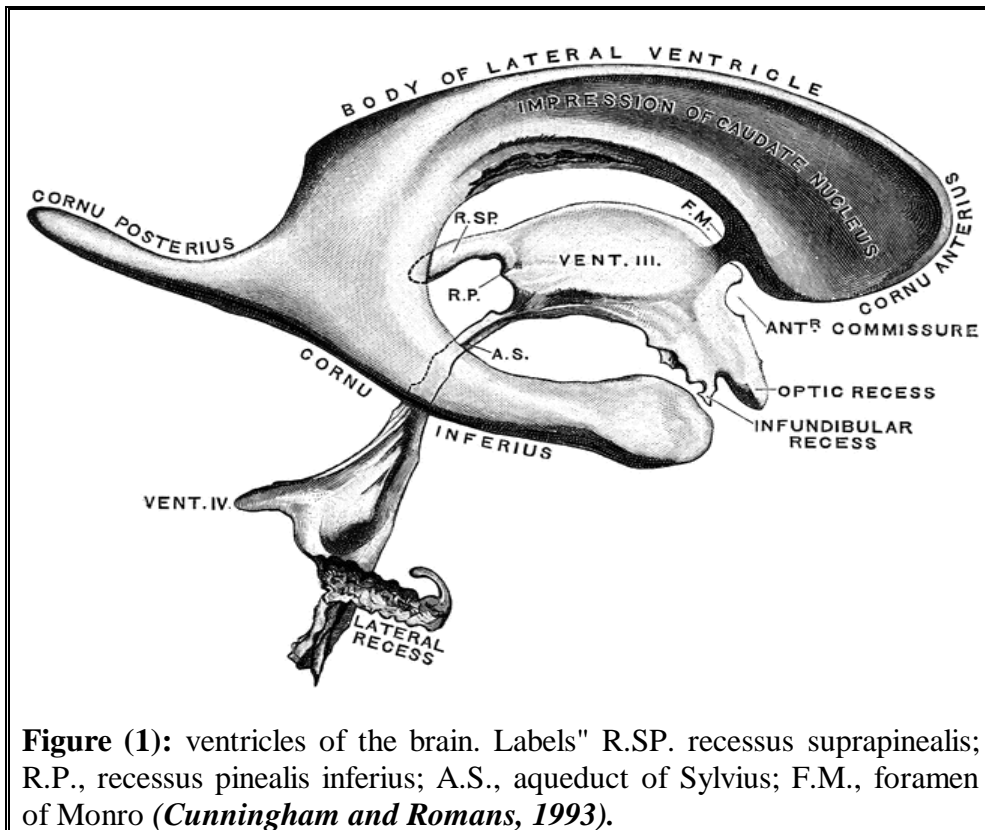


Figure (1): ventricles of the brain. Labels" R.SP. recessus suprapinealis; R.P., recessus pinealis inferior; A.S., aqueduct of Sylvius; F.M., foramen of Monro (*Cunningham and Romans, 1993*).

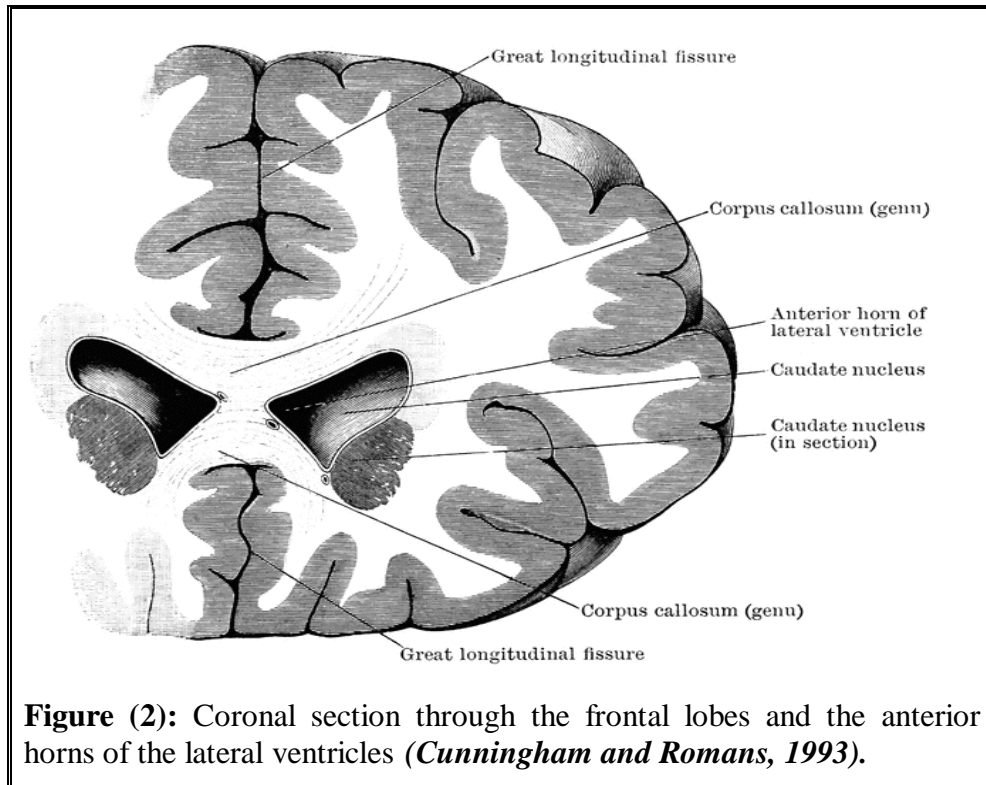
▪ Lateral Ventricle:

Within the cerebral hemisphere lies the lateral ventricle. Viewed from the lateral aspect, the lateral ventricle has a roughly C-shaped profile (*Figure 1*) with an occipital tail. It is divided into a body and frontal (anterior), occipital (posterior) and temporal (inferior) horns.

Frontal (anterior) horns

Passes forward and lateralward from the interventricular foramen into the frontal lobe. Its floor is formed by the upper surface of the corpus callosum. It is bounded medially by the

anterior portion of the septum pellucidum and laterally by the head of the caudate nucleus. Its apex reaches the posterior surface of the genu of the corpus callosum (*figure 2*) (*Ryan and Nicholas, 2004*).



The *body of the lateral ventricle* lies within the frontal and parietal lobes, and extends from the foramen of Monro to the splenium of corpus callosum (*Figure 1*). The bodies of the two ventricles are separated by the septum pellucidum, which contains the columns of the fornices in its lower edge (*Figure 3*). The inferior limit of the body and its medial wall are formed by the body of the fornix. The coronal profile of the body is a flattened triangle with an inward bulging lateral wall formed by